Nuclear Physics B81 (1974) 330–348. North-Holland Publishing Company

ANALYSIS OF $\pi N \to K\Lambda$ AND $\bar{K}N \to \pi\Lambda$ USING FIXED-t DISPERSION RELATIONS, FESR AND DUALITY

R.C.E. DEVENISH
DESY, Hamburg

C.D FROGGATT*
NORDITA, Copenhagen

B R. MARTIN
Department of Physics and Astronomy, University College, London

Received 13 May 1974
(Revised 26 June 1974)

Abstract: A simultaneous analysis of low-energy ($W \leq 2$ GeV) data for the reactions $\pi^- p \to K^0\Lambda$ and $K^- p \to \pi^0\Lambda$ has been made using the hypothesis of two-component duality combined with fixed-t dispersion relations. Results are presented for the $\Sigma^*\Lambda\pi$ and $N^*\Lambda K$ couplings. The low-energy amplitudes are used to evaluate FESR integrals and lead to large EXD breaking for the $K_V^* - K_T^*$ helicity flip amplitudes.

1. Introduction

At low energies, interest in the reactions $\pi N \to K\Lambda$ and $\bar{K}N \to \pi\Lambda$ stems mainly from the information that can be deduced on the spectrum (i.e. masses and total widths) and couplings of N* and Σ^* resonances. In the $S = -1$ channel extensive phase-shift analyses have been made [1] and there is considerable agreement on the form of the spectrum for the more important resonances, although their couplings are less certain. For the $S = 0$ channel, the spectrum is known from analyses of πN scattering, but the N* couplings to $K\Lambda$ are very poorly known because lack of data has hindered phase-shift analysis [2]. The alternative approach of the isobar model [3] assumes resonance saturation for both the real and imaginary parts of the partial wave amplitudes, and although the latter hypothesis is probably a reasonable approximation, the former is almost certainly not. This follows from the fact that whereas the imaginary part of a resonance is a local effect, the real part vanishes at resonance, and is non-negligible some distance from the zero position. These anal-

* Permanent address. Department of Natural Philosophy, University of Glasgow.

yses [3] also, in practice, do not treat correctly the important Born terms (an arbitrary form factor is used to suppress them), and the resulting N* couplings are likely to be unreliable

In the situation where there exists considerable information on the spectrum of N* and Σ^* states it is of interest to explore other methods of determining their couplings A very promising approach in this respect is to use fixed-t dispersion relations and the two-component duality hypothesis [4]. The latter asserts that at low energies the imaginary parts of inelastic two-body amplitudes (i.e those for which pomeron exchange is forbidden in the t-channel) are resonance dominated, and is supported by evidence from πN [5] and KN [6] scattering Fixed-t dispersion relations then enable the real parts to be calculated without additional assumptions about the low-energy imaginary parts The resulting parameterization, by exploiting the constraints from the crossed channel, is very economical In practice the method can be used to extract resonance couplings directly from data, given the resonance spectrum. The resulting amplitudes have fixed-t analyticity by construction. (Amplitudes constructed from conventional phase-shift analysis will not necessarily have this property.) Quantitatively satisfactory results have been obtained from analyses of $\pi^- p \to \pi^0 n$ [7], $\gamma p \to \pi N$ [8] and $\gamma p \to K^+\Lambda$ [9] data.

At high energies line reversed pairs of reactions provide information on the hypothesis of exchange degeneracy (EXD). At present there is little firm evidence on this hypothesis for the $K_V^*(890)$ and $K_T^*(1400)$ pair [10]. A reliable evaluation of finite-energy sum rules (FESR) could help here, but for overall consistency it is essential that the low-energy amplitudes used as input should also fit the low-energy data. Thus, if resonance saturation is used for the imaginary parts in the FESR integrals then these imaginary parts alone should fit the low-energy data. The output amplitudes from our low-energy analysis will conform to this requirement.

In sect. 2 we discuss briefly the fixed-t dispersion relation formalism for $\pi N \to K\Lambda$ and $\bar{K}N \to \pi\Lambda$, and describe the resonance parametrization used. In sect 3 we list the data fitted, and in sect. 4 we discuss the fit to the data and the output low-energy amplitudes. In sect. 5 we evaluate FESR integrals and comment on the implications of the results for $K_V^* - K_T^*$ EXD and high-energy models. Our conclusions are summarized in sect 6.

2. Formalism

2.1 Fixed-t dispersion relations

We work with the usual spin-0 – spin-$\frac{1}{2}$ invariant amplitudes A and B, and denote those for $\pi^- p \to K^0\Lambda$ by A_- and B_-, and those for the crossed reaction $\bar{K}^0 p \to \pi^+\Lambda$ by A_+ and B_+. We choose the 'baryon first' phase convention of Levi-Setti [11] and the Particle Data Group [12], so that our meson state phase factors [13] are different to those of Field and Jackson [14]. Therefore our invariant amplitudes are con-

sistently of the opposite sign to those of ref. [14]. In terms of the variable $\nu \equiv \frac{1}{4}(s-u)$ crossing takes the form

$$A_+(\nu, t) = -A_-(-\nu, t), \qquad B_+(\nu, t) = B_-(-\nu, t).$$

Dispersion relations for $A_\pm$ and $B_\pm$ may be obtained by using a contour consisting of the real axis $|\mathrm{Re}\,\nu| < \nu_c$ and a circle of radius $|\nu| = \nu_c$. They are

$$\pm \mathrm{Re}\,A_\pm(\nu, t) = \frac{1}{\pi}\int_{\nu_+}^{\nu_c} d\nu' \frac{\mathrm{Im}\,A_+(\nu', t)}{\nu' \mp \nu} - \frac{1}{\pi}\int_{\nu_-}^{\nu_c} d\nu' \frac{\mathrm{Im}\,A_-(\nu', t)}{\nu' \pm \nu}$$
$$\pm \frac{1}{2\pi i}\oint_{\nu_c} d\nu' \frac{A_\pm(\nu', t)}{\nu' - \nu} \pm A_\pm^{\mathrm{P}}(\nu, t), \tag{2.1}$$

$$\mathrm{Re}\,B_\pm(\nu, t) = \frac{1}{\pi}\int_{\nu_+}^{\nu_c} d\nu' \frac{\mathrm{Im}\,B_+(\nu', t)}{\nu' \mp \nu} + \frac{1}{\pi}\int_{\nu_-}^{\nu_c} d\nu' \frac{\mathrm{Im}\,B_-(\nu', t)}{\nu' \pm \nu}$$
$$+ \frac{1}{2\pi i}\oint_{\nu_c} d\nu' \frac{B_\pm(\nu', t)}{\nu' - \nu} + B_\pm^{\mathrm{P}}(\nu, t), \tag{2.2}$$

where

$$\nu_- = \tfrac{1}{2}[(N+\mu)^2 - \tfrac{1}{2}\Omega + \tfrac{1}{2}t],$$

$$\nu_+ = \tfrac{1}{2}[(\Lambda+\mu)^2 - \tfrac{1}{2}\Omega + \tfrac{1}{2}t],$$

$$\Omega = K^2 + \mu^2 + N^2 + \Lambda^2,$$

and K, μ, N and Λ are the masses of the kaon, pion, nucleon and lambda, respectively. The pole (Born) terms in (2.1) and (2.2) are given by

$$\pm A_\pm^{\mathrm{P}}(\nu, t) = \left(\frac{2}{3}\right)^{\frac{1}{2}} \frac{N-\Lambda}{4} \frac{G_{\pi\mathrm{NN}} G_{\mathrm{KN}\Lambda}}{\nu_{\mathrm{N}} + \frac{1}{4}t \pm \nu} - \frac{2\Sigma - \Lambda - N}{4} \frac{G_{\pi\Lambda\Sigma} G_{\mathrm{KN}\Sigma}}{\nu_\Sigma + \frac{1}{4}t \mp \nu}$$

$$B_\pm^{\mathrm{P}}(\nu, t) = \left(\frac{2}{3}\right)^{\frac{1}{2}} \frac{1}{2} \frac{G_{\pi\mathrm{NN}} G_{\mathrm{KN}\Lambda}}{\nu_{\mathrm{N}} + \frac{1}{4}t \pm \nu} + \frac{1}{2} \frac{G_{\pi\Lambda\Sigma} G_{\mathrm{KN}\Sigma}}{\nu_\Sigma + \frac{1}{4}t \mp \nu},$$

where

$$\nu_i = \tfrac{1}{4}(2M_i^2 - \Omega), \qquad i = \mathrm{N}, \Sigma,$$

and the G's are coupling constants in the normalization and 'baryon first' phase convention of Levi-Setti [11]. They are related to the usual [15] charge-independent couplings g by

$$G_{\pi NN} = \sqrt{3}\, g_{\pi NN}\,, \qquad G_{\pi\Lambda\Sigma} = g_{\pi\Lambda\Sigma}\,,$$
$$G_{KN\Lambda} = g_{KN\Lambda}\,, \qquad G_{KN\Sigma} = \sqrt{2}\, g_{KN\Sigma}\,. \tag{2.3}$$

To evaluate eqs. (2.1) and (2.2) for those cases where convergence is obtained as $\nu_c \to \infty$ requires a knowledge of the imaginary parts for $\nu' > \nu_c$. Expectations based on the assumed dominance of $K_V^* - K_T^*$ exchange at high energies suggest that not all the dispersion relations will converge, and in at least one case we would need a model for the entire amplitude on the circle $|\nu'| = \nu_c$. For simplicity, we have treated both cases in the same phenomenological way by representing the high-energy part of the dispersion relation by an integral over a small number of 'pseudo-resonances' [8] of fixed masses $W_R > 2$ GeV (i.e. above the region of fitted data), but variable couplings. The consistency of this procedure is discussed in sect. 4.

The low-energy imaginary parts are expressed as sums of resonances of fixed masses and widths but free couplings (the necessary partial wave decompositions are given in ref. [14]), and it is these couplings, together with those of the Born terms and the 'pseudo-resonances', that are the parameters of the model.

2.2. Resonance parametrization

The general resonance formula we use for the imaginary part of a partial wave amplitude is

$$\operatorname{Im} f_{l\pm}^{IJ}(W) = \frac{(\Gamma_i \Gamma_j)^{\frac{1}{2}}}{2(k_i k_j)^{\frac{1}{2}}} \frac{\frac{1}{2}\Gamma}{(W_R - W)^2 + (\frac{1}{2}\Gamma)^2}\,, \tag{2.4}$$

where $W = \sqrt{s}$; W_R is the mass of the resonance of total width Γ and partial width Γ_i, Γ_j into channel i, j, and k_i, k_j are the c.m. momenta in the two channels.

To achieve the correct threshold behaviours at each of the thresholds we have inserted simple barrier factors into the widths. However, since these are not expected to play a significant role above the resonance energy, we have set them equal to unity for all $W \geqslant W_R$. We distinguish two cases. (i) a resonance occurring between two thresholds (e.g. the $P_{11}N(1470)$, which lies between the πN and $K\Lambda$ thresholds), and (ii) a resonance lying above the highest threshold (e.g. the F_{15} $\Sigma(1910)$, which lies above both the $\pi\Lambda$ and $\bar{K}N$ thresholds). The appropriate modifications to the partial widths for the various regions in both cases are obtained by analytic continuation, and are given in table 1. We take the momentum dependence of the total width to be that of the lowest mass channel. Using the results of this table it is straightforward to show that the contribution of a resonance to $\operatorname{Im} A_\pm$ and $\operatorname{Im} B_\pm$ is a real continuous function having the required threshold behaviours at both thresholds.

Table 1
Forms used for $\Gamma_i(k_i)$ and $\Gamma_j(k_j)$ in eq. (2.4), assuming that the threshold for channel i is below that for channel j

Resonance between thresholds			Resonance above both thresholds		
region	Γ_i	Γ_j	region	Γ_i	Γ_j
$k_i > k_i^R$ $k_j > \lvert k_j^R \rvert$	γ_i	γ_j	$k_i > k_i^R$ $k_j > k_j^R$	γ_i	γ_j
$k_i > k_i^R$ $k_j < \lvert k_j^R \rvert$	γ_i	$\gamma_j \left(\frac{k_j}{\lvert k_j^R \rvert} \right)^{2l+1}$	$k_i < k_i^R$ $k_j < k_j^R$	$\gamma_i \left(\frac{k_i}{k_i^R} \right)^{2l+1}$	$\gamma_j \left(\frac{k_j}{k_j^R} \right)^{2l+1}$
$k_i > k_i^R$ $\lvert k_j \rvert < \lvert k_j^R \rvert$	γ_i	$\gamma_j \left(\frac{i\lvert k_j \rvert}{\lvert k_j^R \rvert} \right)^{2l+1}$	$k_i < k_i^R$ $\lvert k_j \rvert < k_j^R$	$\gamma_i \left(\frac{k_i}{k_i^R} \right)^{2l+1}$	$\gamma_j \left(\frac{i\lvert k_j \rvert}{k_j^R} \right)^{2l+1}$
$k_i < k_i^R$ $\lvert k_j \rvert > \lvert k_j^R \rvert$	$\gamma_i \left(\frac{k_i}{k_i^R} \right)^{2l+1}$	$\gamma_j i^{2l+1}$	$k_i < k_i^R$ $\lvert k_j \rvert > k_j^R$	$\gamma_i \left(\frac{k_i}{k_i^R} \right)^{2l+1}$	$\gamma_j i^{2l+1}$

Centre-of-mass momenta at the resonance energy $W = W_R$ are denoted k_i^R, k_j^R, and the moduli signs imply that the momentum has been analytically continued below the channel threshold. The quantities γ_i, γ_j are real coupling constants.

3. Data

For the $S = 0$ channel, $\pi^- p \to K^0\Lambda$, we have fitted all available differential cross section (dcs) and polarization (P) data for $W \lesssim 2$ GeV (this corresponds to $k_{lab} \lesssim 1.6$ GeV/c), and $|t| \lesssim 1$ GeV^2. The range in t is based on a conservative estimate of the range of validity of the relevant partial wave expansions. The data were taken from ref. [16], and consist of 307 dcs, 81 P and 84 P' dcs measurements.

In the $S = -1$ channel, $\bar{K}^0 p \to \pi^+\Lambda$, there are essentially no data available. The isospin related channel $K^- p \to \pi^0\Lambda$ has, however, been extensively studied, and so we have used data for this reaction. Since the sum total of data available for $K^- p \to \pi^0\Lambda$ far exceeds that for $\pi^- p \to K^0\Lambda$, and in order that the $S = -1$ data should not dominate the solution, we have restricted ourselves to the representative data of ref. [17], which consists of 916 dcs, 294 P and 104 P' dcs measurements. More $S = -1$ data can be included when they can be balanced by more experiments on $\pi^- p \to K^0\Lambda$. The total number of data points is 1786.

4. Low-energy amplitudes

The low-energy input spectrum used is shown in table 2 The criterion used to select the Σ^* spectrum was that it should include all states listed as 'two star' and above in the Particle Data Group tables [12] with respect to the $\pi\Lambda$ decay channel The N^* spectrum decaying into the $K\Lambda$ channel is much less understood, and we have selected all N^* resonances with an overall 'two star' or better status. The masses and total widths are as given in ref. [12]. For the 'pseudo-resonances' we made no serious attempt to identify them with actual particles, but have included some which have been suggested in recent analyses [12, 19].

For a set of couplings for the Born terms and the resonances, the imaginary parts of $A_\pm$ and $B_\pm$ were obtained by the usual partial wave series, and the real parts found by evaluating the dispersion relations (2.1) and (2.2) The couplings were varied to fit the data described in sect. 3. Numerous solutions have been investigated using as initial estimates for the couplings values obtained from phase-shift analyses [1, 2, 19, 20], as well as predictions from symmetry schemes [11, 14, 19, 22]. The overall best solution has $\chi^2/\mathrm{NDF} = 2.28$, and gives a good representation of the data, comparable to other energy-dependent fits to more than a single channel. As examples of the quality of the solution we show in figs. 1 and 2 fits to a sample of the data in each channel. A breakdown of the final χ^2 by channel and data type is shown in table 3.

Table 2
Input spectrum of N^* and Σ^* resonances used in the fixed-t dispersion relations

N^* resonances			Σ^* resonances		
resonance	mass (MeV)	total width (MeV)	resonance	mass (MeV)	total width (MeV)
P_{11}	1470	240	P_{13}	1383	36
S_{11}	1530	70	D_{13}	1670	50
D_{13}	1520	120	S_{11}	1750	65
D_{15}	1672	142	D_{15}	1765	120
F_{15}	1688	127	P'_{13}	1840	100
S'_{11}	1706	140	F_{15}	1910	70
D'_{13}	1730	130	P_{11}	1926	185
P'_{11}	1783	250	D'_{13}	1940	200
P_{13}	1864	335	F_{17}	2030	135
F_{17}	1990	200			
D''_{13}	2046	243	P''_{13}	2070	100
G_{17}	2184	275	G_{17}	2100	100
			$H_{1\,11}$	2210	100
H_{19}	2220	260	P'''_{13}	2290	150

'Pseudo-resonances' used to parameterise the high-energy region are shown below the dashed line

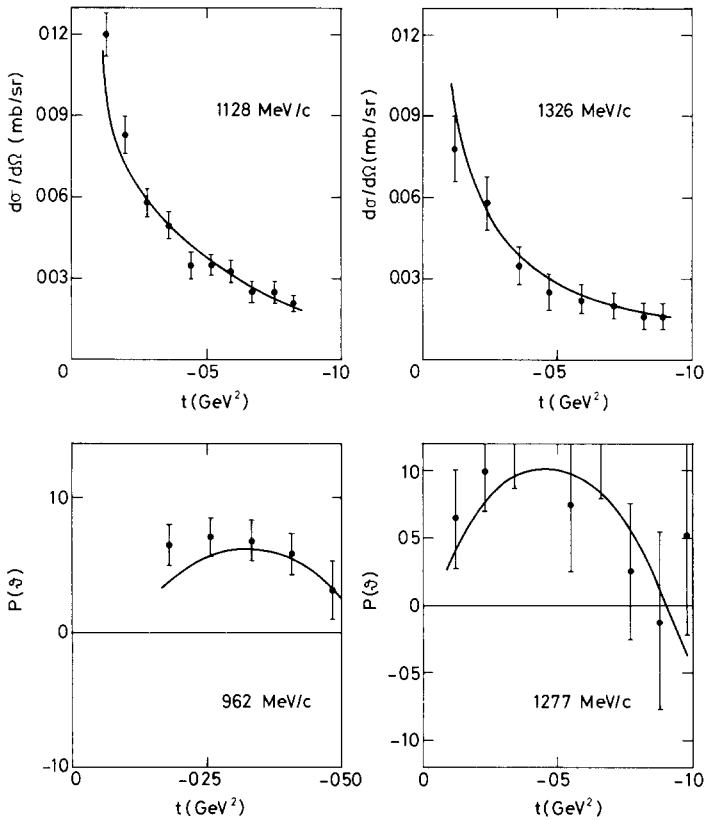

Fig. 1. Fits to sample differential cross section and polarization data for $\pi^- p \to K^0\Lambda$.

The couplings of the low-energy resonances $(\Gamma_l\Gamma_J)^{\frac{1}{2}}$ and the Born terms $G_l G_J/4\pi$ are given in table 4. Following Levi-Setti [11] the partial widths include all charge modes and are related to the amplitude at resonance t_{IJ}, usually quoted in phase-shift analysis [12], by

$$(\Gamma_l\Gamma_J)^{\frac{1}{2}} = t_{IJ}\Gamma ,$$

while the couplings G_l are related to the usual [15] charge-independent ones by eq. (2.3). The errors are estimates of how much each parameter can be varied to produce a change in χ^2 of 2.5%, after reminimising on the remaining parameters. (A change much greater than this begins to produce qualitative differences in the solu tion.) A point of importance for what follows is that in all solutions the couplings of the Born terms and the P_{13} $\Sigma(1385)$ were always found to be well within the errors quoted.

The most recent reviews [19, 20] of $\bar{K}N \to \pi\Lambda$ partial wave analysis conclude that the D_{13} $\Sigma(1660)$, S_{11} $\Sigma(1750)$, D_{15} $\Sigma(1765)$, F_{15} $\Sigma(1915)$ and F_{17} $\Sigma(2030)$

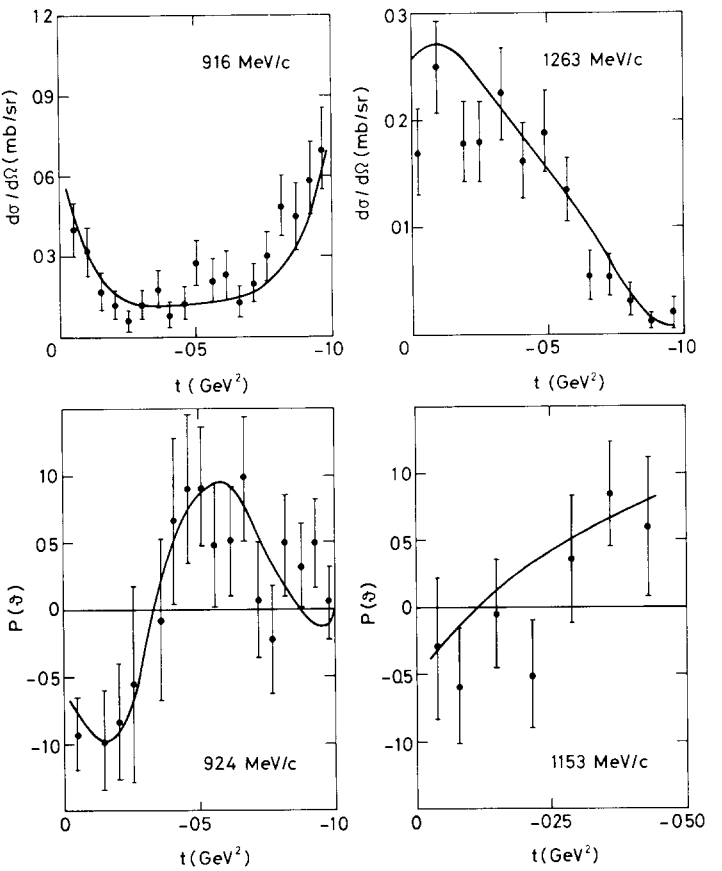

Fig. 2. Fits to sample differential cross section and polarization data for $K^-p \to \pi^0\Lambda$.

Table 3
Breakdown of the χ^2/N data by channel and data type for the final solution listed in tables 4 and 5

Channel		DSC	P	$P \times$ DCS	Total
$\pi^-p \to K^0\Lambda$	no. of data	307	81	84	472
	χ^2/N data	2.6	2.0	3.48	2.66
$K^-p \to \pi^0\Lambda$	no. of data	916	294	104	1314
	χ^2/N data	2.4	1.68	1.21	2.15

Table 4
Values of the couplings $(\Gamma_l \Gamma_j)^{\frac{1}{2}} = t_{ll'} \Gamma$ at resonance in MeV, and of the Born couplings $G_l G_j / 4\pi$ (dimensionless) from this analysis compared with values used in recent FESR evaluations [14, 18], and estimates from phase-shift analyses (see text)

	State	This calculation	Ref. [14]	Ref. [18]	PSA
	N(938)	−17.6 ± 6.8	−24.1	−24.1	
	$P_{11}(1470)$	−71.1 ± 16.3	−40	−40	
	$S_{11}(1530)$	−48.4 ± 15.0	5.5	3.8	
	$D_{13}(1520)$	− 9.1 ± 3 8	− 7.2	− 7.2	
	$D_{15}(1672)$	− 4.8 ± 0.9	− 2.2	0 or 4.8	− 3 ± 3
N*	$F_{15}(1688)$	− 1.1 ± 1.1	− 1.2	0	− 2 ± 2
	$S'_{11}(1706)$	−25.0 ± 4 6	−41.6	−24.7	−29 ± 4
	$D'_{13}(1730)$	3 4 ± 2.5			
	$P'_{11}(1783)$	−37.4 ± 9.6	13.5	6.1	−34 ± 8
	$P_{13}(1864)$	−22 3 ± 11.2	−18.1	− 8.6	−34 ± 7
	$F_{17}(1990)$	− 4 2 ± 6.6			
	Σ(1189)	− 7.1 ± 1.9	− 5.7	− 5.7	
	$P_{13}(1383)$	21.1 ± 11.5	17	27	
	$D_{13}(1670)$	0.9 ± 3.0	5	6.8	3 ± 1
	$S_{11}(1750)$	− 7.8 ± 5.0	−20	−23	− 9 ± 4
	$D_{15}(1765)$	−31.1 ± 5.7	−27	−75	−42 ± 10
Σ*	$P'_{13}(1840)$	12.2 ± 7.8			4 to 24
	$F_{15}(1910)$	− 6.1 ± 3 9	− 4.9	−15.1	− 9 ± 3
	$P_{11}(1926)$	−31.3 ± 22.0	−24	−36	−24 to +11
	$D_{13}(1940)$	−30.5 ± 13.9	−39.2 [a]	−26.4	− 8 to −40
	$F_{17}(2030)$	26.3 ± 7 1	34	− 7.8	36 ± 4

[a] This state was actually omitted in most of the calculations of ref. [14].
Phases and normalizations have been changed to agree with the Levi-Setti conventions [11] where necessary.

resonance parameters are reasonably well established We therefore list in table 4 the couplings for these five resonances from Van Horn's analysis [21], as given in table 7 of ref [19].

The three remaining above-threshold states, P_{13} Σ(1840), P_{11} Σ(1926), and D_{13} Σ(1940) have considerable associated background, and we list ranges for their couplings from refs. [12, 19]. There is much less information on N* resonance parameters from $\pi N \to K\Lambda$ partial wave analyses [2], and we give average values for the couplings of the D_{15} N(1672), F_{15} N(1688), S_{11} N(1706), P_{11} N(1783), and P_{13} N(1864). In addition, solution B of Lovelace and Wagner [2] contains a D_{13} N(1730) with a coupling $t\Gamma \approx 15$ MeV.

Information on the couplings of the below-threshold states is, of course, much less direct, and comes almost exclusively from SU(3) fits [11, 12, 19] to decay rates,

Table 5
Values of the couplings $(\Gamma_i \Gamma_j)^{\frac{1}{2}} = t_{ij}\Gamma$ at resonance (in MeV) for the 'pseudo-resonances'

N* resonance		Σ* resonances	
state	coupling	state	coupling
$D'_{13}(2046)$	9.3	$P''_{13}(2070)$	23.9
$G_{17}(2184)$	15.4	$G_{17}(2100)$	−27.6
$H_{19}(2220)$	− 7.2	$H_{1\,11}(2210)$	−12.0
		$P'''_{13}(2290)$	30.0

or higher symmetry estimates. This is the source of the values quoted in refs. [14] and [18] and of their Born term couplings (calculated from SU(3) with $\alpha = D/(D+F) = 0.6$). The least reliable of the SU(3) estimates are those for the S_{11} N(1530) and P_{11} N(1470). In particular, for the former, the most recent SU(3) fits [12, 19] give $t\Gamma \approx -2$ MeV, while $SU(6)_W$ fits [22] including mixing with the S_{11} N(1706) give $t\Gamma \approx -30$ MeV. The latter is in agreement with our own estimate (see table 4).

The agreement between our results and those from phase shift analysis is very encouraging Also our values for the P_{13} Σ(1383) and Born term couplings are in remarkably good agreement with SU(3) considering the difficulty of including these large pole terms properly in isobar models [3]. The direction of SU(3) breaking for the Born couplings is even such as to reduce the coupling to a value close to that obtained in the most reliable of previous phenomenological estimates [15, 23]. Also shown in table 4 are values of the couplings used in two recent FESR evaluations [14, 18], which we will comment on in sect 5 below.

The values of the couplings of the 'pseudo-resonances' are given in table 5. Although we have not tried to identify these with physical states (table 5 is presented solely that the amplitudes to be discussed below can be reproduced) we have checked that the resulting high energy contributions to the low-energy region, and the total imaginary parts near the cutoff $\nu = \nu_c$ are both consistent with expectations from high energy models To do this we have used the models of Loos and Matthews [24], Irving et al. [25], and Field and Jackson [14], and to calculate the contributions to the low energy region we have evaluated the contour integrals in eqs. (2.1) and (2.2). We find that the 'pseudoresonances' give total contributions whose order of magnitude is consistent with the contour integrals, and whose total imaginary parts near $\nu = \nu_c$ are also qualitatively consistent with those of the high-energy models.

In figs. 3 and 4 we show the low-energy amplitudes $A'_{\pm}(\nu, t)$ and $B_{\pm}(\nu, t)$, the former defined by

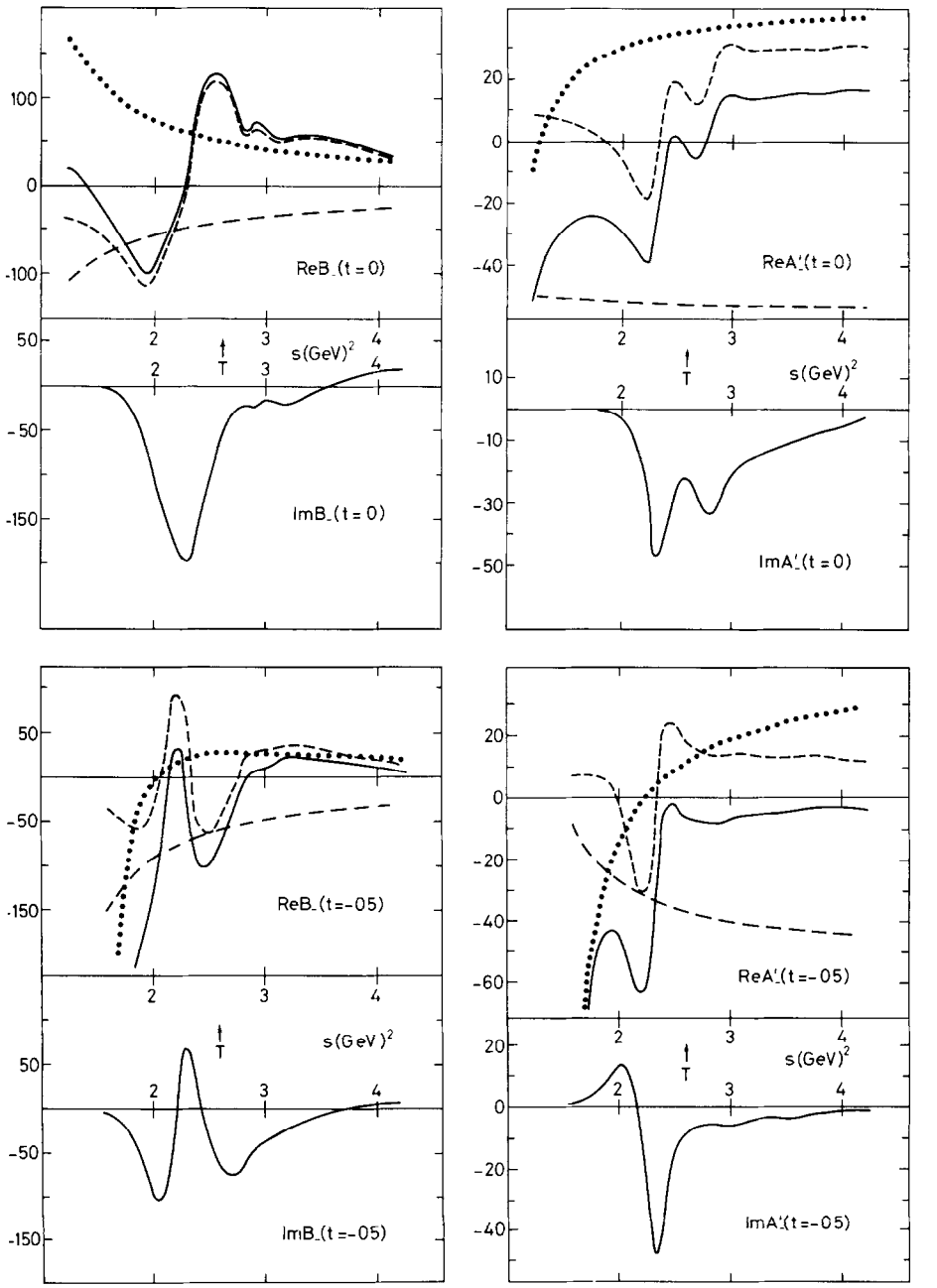

Fig. 3. Values of $A'_-(\nu, t)$ and $B_-(\nu, t)$ for $t = 0$ and -0.5 GeV^2 in units GeV = 1. The various contributions are (– – –)N*, (–·–·–)Σ*, (. . .)Born, (——)total. The physical threshold is denoted by T.

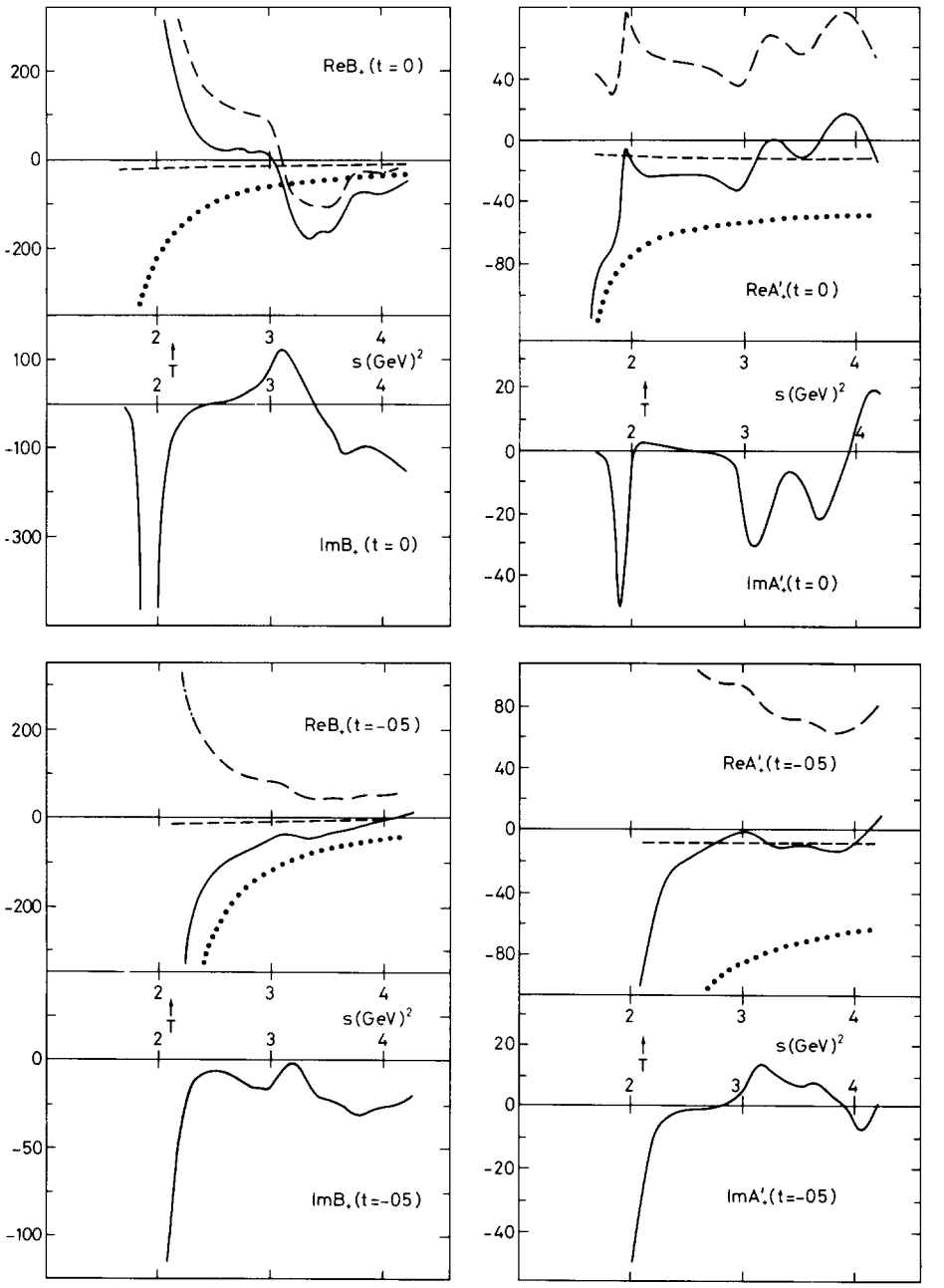

Fig. 4. Values of $A'_+(\upsilon, t)$ and $B_+(\upsilon, t)$ for $t = 0$ and -0.5 GeV^2 in units GeV = 1. The various contributions are. (– – –)N^*, (–·–·–)Σ^*, (. . .)Born, (——) total. The physical threshold is denoted by T.

Table 6
Individual contributions of physical region resonances to the integrated cross section compared to data

	Resonance	Mass (MeV)	p_L (approx) (GeV/c)	σ_T(res)	$\sigma_T(\pi^- p \to K^0\Lambda)$
			0.904		0 056 ± 0.015
	D_{15}	1672	1.0	0.036	0.56 ± 0.04
	F_{15}	1688	1.03	0.003	0.73 ± 0.03
	S'_{11}	1706	1.06	0 31	0.899 ± 0.06
N*	D'_{13}	1730	1.11	0.012	0.58 ± 0.034
	P'_{11}	1783	1.205	0.181	0.29 ± 0.05
	P_{13}	1864	1.36	0.061	0.3 ± 0.05
	F_{17}	1990	1.62	0.01	0.21 ± 0.025
					$\sigma_T(K^- p \to \pi^0\Lambda)$
			0.293		5.2 ± 0 9
	D_{13}	1670	0 74	0.009	2.43 ± 0.38
	S_{11}	1750	0.91	0.15	3.4 ± 0.3
	D_{15}	1765	0.94	1.97	2.9 ± 0.24
	P'_{13}	1840	1.1	0.233	1.69 ± 0.15
Σ^*	F_{15}	1910	1 25	0.147	~1.25 ± 0.1
	P_{11}	1926	1.29	0.178	~1.2 ± 0.08
	D_{13}	1940	1.32	0.288	1.12 ± 0.14
	F_{17}	2030	1.52	0.758	~1.15 ± 0.06

The data are taken from CERN/HERA 72–1 and 2 σ_T is in mb

$$A'_{\pm}(\nu, t) \equiv \left[1 - \frac{t}{(\Lambda + N)^2}\right] A_{\pm}(\nu, t) + \left[\frac{2\nu}{\Lambda + N} + \frac{(\Lambda - N)(\mu^2 - K^2)}{2(\Lambda + N)^2}\right] B_{\pm}(\nu, t) \tag{4.1}$$

for $t = 0$ and -0.5 (GeV)^2. These amplitudes are essentially the t-channel helicity amplitudes [14], and have been calculated using *all* the states of table 2.

For the real parts of the $\pi^- p \to K^0\Lambda$ amplitudes (fig. 3) the main feature is a strong cancellation between the Σ^*'s (of which the dominant contribution is the $P_{13}(1383)$) and the Born terms. The cancellation is almost complete in B and produces a negative background to the N*'s in A' Of the N*'s, the below threshold $P_{11}(1470)$ gives the largest contribution to both the real and imaginary parts. We agree with the results of Lovelace and Wagner [2] that the $S'_{11}(1706)$ and $P'_{11}(1783)$ provide the biggest physical region effects. The $P_{13}(1864)$ is also quite important. The 'importance' of a resonance in the physical region can be judged from table 6 where we show the contribution of individual resonances to the integrated cross section compared to data.

The cancellation between the Born terms and the Σ^*'s is also apparent in the real parts of the $\bar{K}^0 p \to \pi^+\Lambda$ amplitudes (fig. 4), particularly in A'. The background from the N*'s is small. Of the Σ^*'s again the below threshold state $P_{13}(1383)$ provides

the dominant contribution to both real and imaginary parts. As can be seen from fig. 4 and table 6 the physical region states are more important in this channel, particularly the $D_{15}(1765)$ and $F_{17}(2030)$.

The breakdown of the amplitudes discussed above and the results in table 6 show quite clearly the power of the fixed-t method in being able to *calculate* the background.

5. Finite energy sum rules

Using our amplitudes we now examine the behaviour of the low-energy FESR integrals. We work at fixed t with invariant s-channel amplitudes $f_{+\pm}(\nu, t)$ defined by

$$f_{++} \equiv A + \frac{2\nu}{\Lambda + N} B, \qquad f_{+-} \equiv A \tag{5.1}$$

These are proportional, to leading order in s, to the s-channel helicity amplitudes. Combinations corresponding to the exchange of K_V^* and K_T^* quantum numbers in the t-channel are

$$A^{V} \equiv -\tfrac{1}{2}(A_+ + A_-)\,, \qquad A^{T} \equiv -\tfrac{1}{2}(A_+ - A_-)\,, \tag{5.2}$$

(similarly for $B^{V,T}$) and to ensure that we have a function which is odd under crossing we define (dropping helicity indices)

$$F^{V,T}(\nu, t) \equiv \nu^n f^{V,T}(\nu, t)\,, \tag{5.3}$$

where for $K_V^*(K_T^*)$ exchange $n = 0$ (1). The low-energy parts of the FESR integrals are then

$$L^{V,T}(t, k) \equiv \frac{1}{\nu_1^{n+k+1}} \int_0^{\nu_1} \mathrm{d}\nu\, \mathrm{Im}\{(\bar{\nu}^2 - \nu^2)^{\frac{1}{2}k} F^{V,T}(\nu, t)\}\,, \tag{5.4}$$

where the Born terms have been formally included in the integral. We will comment on the choice of the branch point $\bar{\nu}$ below

The idea of evaluating the L's is that they contain information on $F(\nu, t)$ for $\nu \lesssim \nu_1$. In the cases where Regge-pole behaviour $F(\nu) \sim \nu^\alpha$ sets in for the imaginary (real) part for $\nu \gtrsim \nu_1$, $k = 0(1)$ yields information on Im F(Re F) for $\nu > \nu_1$. We do not necessarily expect all the amplitudes to be well approximated by Regge-pole forms. Without a specific model we cannot deduce detailed features at high energies. Nevertheless general features, such as the presence of fixed-t zeros, the order of magnitude of F, and also roughly what its phase is, should be deducible. These have implications for general questions such as the peripherality of tensor exchanges, and the validity of EXD.

To perform the integrations in (5.4) we need the amplitude in the unphysical region. For $k = 0$ we need only Im F; for $k = 1$ we need Im F for $\nu^2 < \bar{\nu}^2$ and Re F for $\nu^2 > \bar{\nu}^2$. We have chosen to use the conventional Legendre series expansions for

the extrapolations. The convergence of these are, strictly speaking, very limited, and governed by the boundaries of double spectral functions. The effective boundaries, however, are given by box graphs with resonance intermediate states, and since these are far from the region of interest it is reasonable to use Legendre series expansions for Im F out to at least $-t = 1$ GeV^2. For Re F the convergence is still, in principle, limited to $|t| \lesssim (\mu + K)^2$, the lowest asymptotic limit of the boundaries of the box graphs. For this reason we have chosen to work with the branch point $\bar{\nu} = \nu_b(t)$ where $\nu_b(t)$ is the largest of the ν values at the physical boundaries of the two reactions $\pi N \to K\Lambda$ and $\bar{K}N \to \pi\Lambda$. This ensures that we need Re F only in the physical region.

The quantities $L_{+,\pm}^{V,T}$ were evaluated using as input the low-energy solution of table 4, i.e. choosing the cutoff ν_1 to exclude the 'pseudo-resonances'. (The low-energy couplings are much better determined than the high-energy ones.) In practice this corresponds to taking $\nu = \nu$ ($W = 2.14$ GeV). In making this evaluation, Re F under the FESR integral is obtained from the fixed-t dispersion relations using the full spectrum of table 2. This is to ensure consistency with the amplitudes obtained from fitting the low-energy data. The results for $k = 0$ are shown by the solid lines on fig. 5. Also shown is an error corridor obtained using the errors given in table 4,

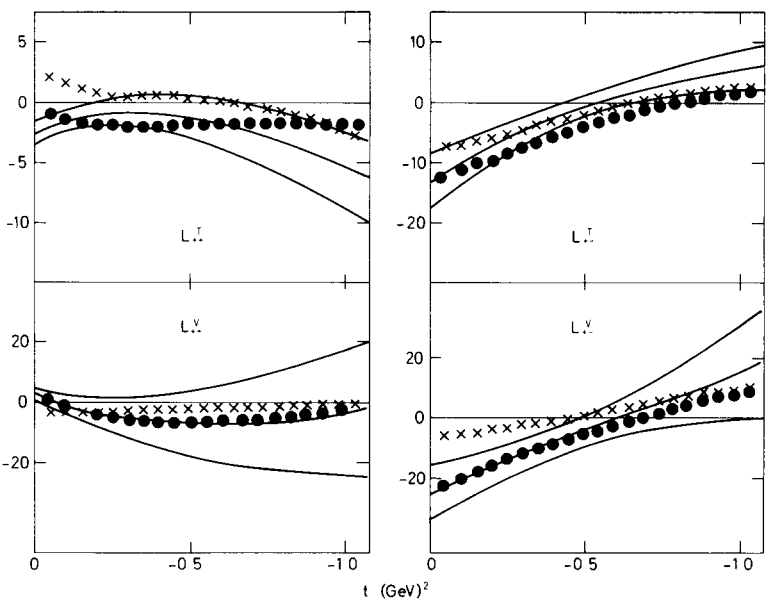

Fig. 5. Values of $L_{+,\pm}^{V,T}(t, k)$. The solid lines give the central values and error corridors for $k = 0$ evaluated with the cutoff corresponding to $W_1 = 2.14$ GeV. The circles show the effect of increasing the cutoff to $W_1 = 2.50$ GeV. The crosses denote the values of L for $k = 1$ using $W_1 = 2.14$ GeV. Units are GeV = 1.

assuming them to be uncorrelated. While this is undoubtedly incorrect quantitatively, it should give a qualitative measure of the relative uncertainties. The results for $k = 1$ are shown by the crosses The errors (not shown) are large because of cancellations in the real parts.

In an EXD Regge pole model, the imaginary parts of both flip amplitudes would have single zeros at $\alpha(t) = 0$, which for

$$\alpha(t) = 0.35 + 0.82t\ , \tag{5.5}$$

(the trajectory passing through the K_V^* and K_T^* masses) is at $t \approx -0.4$ GeV^2. Both the flip terms $L_{+-}^{V,T}(t, 0)$ do indeed show single zeros, but closer to $t = -0.6$ GeV^2, i.e. near the position implied by peripherality, or the dual absorption model [26]. This is consistent with the fact that in both cases the N* and Born contributions are very small, and the t-dependence is essentially that of the Σ^* resonances (although in the case of $L_{+-}^{T}(t, 0)$ the zero is moved in from $t \approx -1.0$ GeV^2 by cancellation between the Σ^*'s and the other contributions). The most important Σ^*'s are the P_{13} $\Sigma(1383)$, D_{15} $\Sigma(1765)$, F_{15} $\Sigma(1910)$, and the F_{17} $\Sigma(2030)$, all of which individually exhibit a peripheral zero at $t \approx -0.5$ (GeV)^2. The quantities $L_{+-}^{V,T}(t, 1)$ however, also show single zeros which is unexpected in any model

Duality and EXD predict that the $S = -1$ amplitude is real at high energies, which in our convention (see eq. (5.2)) implies that $L_{+-}^{V}(t, 0)$ and $L_{+-}^{T}(t, 0)$ should have opposite signs, whereas our results show that these two quantities have the same sign throughout the entire t range Thus the imaginary parts of the flip amplitudes, while consistent with a peripheral picture [26] are not consistent with the hypothesis that they are dominated by EXD Regge poles. This conclusion has also been reached by Vanryckeghem in a recent evaluation of FESR integrals for hypercharge exchange reactions [27]. The EXD breaking is in the same direction as suggested by data at higher energies [10].

To check whether this conclusion is dependent on the cutoff position we have also evaluated the integrals for $k = 0$ including the 'pseudo-resonances'. Thus we use $\nu_1 = \nu_c = \nu$ ($W = 2.5$ GeV). The results are shown by the circles in fig. 5, and do not change our previous conclusions. This suggests that amplitude analyses which have been made under just this EXD assumption [25] should be re-examined It is interesting that a similar conclusion regarding EXD breaking in the low-energy domain for $\rho - A_2$ exchange helicity flip amplitudes has been obtained in a recent analysis of FESR integrals for KN scattering [28]. This latter analysis also finds a zero in the real part of the tensor flip amplitude at $t \approx -0.6$ GeV^2 (but finds a double zero in the real part of the vector amplitude and no zero in the imaginary part of the tensor amplitude). For the nonflip terms, $L_{++}^{V}(t, 0)$ shows a strong absorption zero [26] at $t \approx -0.1$ GeV^2 with a suggestion of a second zero at larger t values, but the errors are very large there. $L_{++}^{V}(t, 1)$ is very small and shows no zeros. $L_{++}^{T}(t, 0)$ also shows evidence for a zero at small t, but equally valid interpretations are two closely spaced zeros, or possibly a double zero at $t \approx -0.4$ GeV^2. Since $L_{++}^{T}(t, 1)$ has a single zero at $t \approx -0.5$ GeV^2, the latter interpretation is consistent with the 'no-compensation'

mechanism [29]. However, the structure in $L_{++}^{T}(t, 0)$ is not very stable as the cutoff is increased, and so any interpretation is open to question. In both non-flip terms $L_{+}^{V,T}{}_{+}(t, 0)$ there are strong cancellations between the Σ^*'s (mainly the P_{13} $\Sigma(1383)$) and the Born terms, with the resulting t-dependence largely that of the N* resonances. At small t the important N*'s are the $S_{11}(1530)$, $P'_{11}(1783)$ and $P_{13}(1864)$ At large t these are replaced by the $D_{13}(1520)$ and $D_{15}(1672)$.

Overall, the results for the non-flip terms (i.e. $L_{++}^{V}(t, 1)$ small, the 'cross-over' zero in $L_{++}^{V}(t, 0)$, and the zero structures in L_{++}^{T}) are in agreement with the amplitude analysis of Irving et al. [25] at 4 GeV/c despite the fact that the latter authors used input assumptions for the flip amplitudes which are contradicted by our FESR results. This is not too surprising because both in [25] and here the flip amplitudes have a zero near $t = -0.5$ GeV^2. As the flip amplitudes must also vanish in the forward direction they are not important for $|t| \lesssim 0.6$ GeV^2. (See also [25] fig. 8 where experimental bounds are shown for the modulus of the physical flip amplitude and comment on p. 586).

Finally, we compare our results with those obtained in two previous FESR analyses [14, 18]. In the paper of Field and Jackson [14] FESR's for the imaginary parts of the amplitudes A' and B (the former defined in eq. (4.1)) were evaluated in a narrow-width approximation using the input parameters of table 4. These amplitudes are directly related to t-channel helicity amplitudes. By assuming unit slopes (1 GeV^{-2}) for the K_V^* and K_T^* trajectories and defining $\alpha^V(t)$, ($\alpha^T(t)$) to be zero at the position where the sum rule for Im B^V, (Im A'^T) vanishes, the trajectory functions were obtained. The vector and tensor pole residues then follow from sum rules for Im $A'^{V,T}$ and Im $B^{V,T}$. Exchange-degeneracy is claimed for the B (t-channel flip) residues, but the A' (t-channel nonflip) residues differ by a low-order polynomial. However, the trajectories, which exhibit approximate EXD, are found to have very low intercepts $\alpha(0) \approx 0.15$. Repeating the calculations of Field and Jackson with our parameters (without the narrow-width approximation) could give $\alpha^V(0) \approx \alpha^T(0)$ 0.4 a result much closer to the EXD trajectory of eq. (5.5). However in view of the large errors on the integrals we do not consider such a method to be reliable. The results for the sums $A'^{V,T}$ are qualitatively similar to those for $L_{+}^{V,T}{}_{+}(t, 0)$. There is some evidence for EXD in the sums for $B^{V,T}$ in that they have opposite signs. The errors are large, particularly on B^T.

Argyres et al. [18] also examine FESR's for the imaginary parts of Λ hypercharge exchange reactions using s channel amplitudes. They present a solution which exhibits approximate EXD for the flip amplitudes. This is achieved, however, only by choosing unphysical values for the couplings of some of the low-energy resonances, in particular for the important D_{15} $\Sigma(1765)$ and F_{17} $\Sigma(2030)$ (see table 4). This again illustrates the importance of using an input solution which actually reproduces the low-energy data.

6. Conclusions

We have used fixed-t dispersion relations and duality to determine the $\Sigma^*\Lambda\pi$ and $N^*\Lambda K$ couplings from data on the reactions $\pi^- p \to K^0\Lambda$ and $K^- p \to \pi^0\Lambda$. Where comparable our results are in agreement with previous phase-shift analyses (see refs [1, 2]). We also give information on the important below threshold resonances and the Born term couplings. Our results are summarized in tables 3 and 4 By using dispersion relations we are able to calculate the backgrounds.

Using these couplings we have evaluated low-energy FESR intergrals for amplitudes asymptotically proportional to s-channel helicity amplitudes. The results are summarized in fig. 5. In particular we find no evidence for exchange degeneracy in the flip amplitudes. This is in contrast to two recent amplitude analyses [18, 25] where just such an assumption was made. In particular in ref. [18] EXD is enforced for the low-energy integrals by adjusting the resonance couplings. As can be seen from table 4 in many cases their values lie outside the range that we have determined from the low energy data. In view of the size of the errors on the FESR integrals we also consider it most unreliable to determine the trajectory parameters from the positions of the zeros of the integrals as was done in ref. [14].

RCED, CDF and BRM wish to thank DESY, NORDITA and CERN respectively for hospitality during various stages of this work. We thank F.T. Meiere, F. Elvekjaer, C. Michael, R.C. Johnson, A.T. Davies, J.L. Petersen and D.G. Sutherland for discussions.

References

[1] A.J. Van Horn, LBL-1370 (1972) unpuplished,
P.J. Litchfield et al., Nucl. Phys. B30 (1971) 125,
W. Langbein and F. Wagner, Nucl. Phys. B47 (1972) 477,
A.T. Lea, B.R. Martin, R.G. Moorhouse and G.C. Oades, Nucl. Phys. B56 (1973) 77.
[2] S. Orito and S. Sasaki, Nuovo Cimento Letters 1 (1969) 936;
F. Wagner and C. Lovelace, Nucl. Phys. B25 (1971) 411.
[3] J. Rush, Phys. Rev. 173 (1968) 1776, and refs. therein.
[4] P.G.O. Freund, Phys. Rev. Letters 20 (1968) 235,
H. Harari, Phys. Letters 20 (1968) 1395.
[5] H. Harari and Y. Zarmi, Phys. Rev. 187 (1969) 2230.
[6] M. Fukugita and T. Inami, Nucl. Phys. B44 (1972) 490.
[7] R.C.E, Devenish and B.R. Martin, Phys. Rev. D8 (1973) 3126
[8] R.G. Moorhouse and H. Oberlack, Phys. Letters 43B (1973) 44,
R.G. Moorhouse, H. Oberlack and A.H. Rosenfeld, Phys. Rev. D9 (1974) 1.
[9] A.R. Pickering, Nucl. Phys. B66 (1973) 493.
[10] G.C. Fox and C. Quigg, Ann. Rev. Nucl. Sci. 23 (1973) 219.
[11] R. Levi-Setti, Proc. of Lund Conf on elementary particles, 1968.
[12] Particle Data Group, Rev. Mod Phys. 45 (1973) 1.
[13] J.J. de Swart, Rev. Mod. Phys. 35 (1963) 916.

[14] R.D. Field and J.D. Jackson, Phys. Rev. D4 (1971) 693.
[15] H. Pilkuhn et al., Nucl. Phys. B65 (1973) 460.
[16] L.B. Auerbach et al., Nuovo Cimento 47 (1967) 19;
F. Crawford et al., Proc. Kiev Conf. on elementary particles 1969 p. 443,
J.C. Doyle, UCRL-18139 (1969), unpublished,
J.C. Doyle et al., Proc. CERN Conf. on elementary particles (1958), p. 148,
T.O. Binford et al., Phys. Rev. 183 (1969) 1134;
Y.S. Kim et al., Phys. Rev. 163 (1967) 1430,
L. Bertanza et al., Phys. Rev. Letters 8 (1962) 332,
F. Eisler et al. Proc. Aix Conf. on elementary particles, 1961, p. 203;
L.L. Yoder et al., Phys. Rev. 132 (1963) 1778;
J. Keren, Phys. Rev. 133 (1964) B457;
O. Goussu et al., Nuovo Cimento 42A (1966) 606.
[17] R. Armenteros et al., Nucl. Phys. B8 (1968) 233; B21 (1970) 15;
L. Bertanza et al., Phys. Rev. 177 (1969) 2036;
A.J. Van Horn, LBL-1370 (1972), unpublished.
[18] E.N. Argyres, A.P. Contogouris and J.P. Holden, Phys. Rev. D9 (1974) 1340.
[19] I. Butterworth, Proc. 2nd Aix Conf. on elementary particles, 1973, J. de Phys Suppl.
[20] P.J. Litchfield, Proc. 2nd Aix Conf. on elementary particels, 1973, J. de Phys Suppl.
[21] A.J. Van Horn, LBL-1370 (1972), unpublished.
[22] D. Faiman and D.E. Plane, Nucl. Phys. B50 (1972) 379.
[23] E. Pietarinen and C.P. Knudsen, Nucl. Phys. B57 (1973) 637.
[24] J.S. Loos and J.A.J. Matthews, Phys. Rev D6 (1972) 2463.
[25] A.C. Irving, A.D. Martin and V. Barger, Nuovo Cimento 16A (1973) 573.
[26] H. Harari, Ann. of Phys. 63 (1971) 432.
[27] L.G.F. Vanryckeghem, Oxford preprint 14/74, unpublished.
[28] F. Elvekjaer and B.R. Martin, Nucl. Phys. B75 (1974) 388.
[29] C.B. Chiu, S.Y. Chu and L.L. Wang, Phys. Rev. 161 (1967) 1563